

1 **Partitioning of Evapotranspiration Using a Stable Isotope Technique in an Arid and**  
2 **High Temperature Agricultural Production System**

3 Xuefei Lu<sup>1</sup>, Liyin L. Liang<sup>2</sup>, Lixin Wang<sup>1\*</sup>, G. Darrel Jenerette<sup>3</sup>, Matthew F. McCabe<sup>4</sup>  
4 and David A. Grantz<sup>3</sup>

5 <sup>1</sup>Department of Earth Sciences, Indiana University-Purdue University Indianapolis  
6 (IUPUI), IN 46202

7 <sup>2</sup>School of Science, University of Waikato, Hamilton, New Zealand

8 <sup>3</sup>Department of Botany & Plant Sciences, University of California Riverside, Riverside,  
9 CA 92521

10 <sup>4</sup>Water Desalination and Reuse Center, Division of Biological and Environmental  
11 Sciences and Engineering, King Abdullah University of Science and Technology,  
12 Thuwal, Saudi Arabia

13

14

15 \*Corresponding author

16 Lixin Wang

17 Department of Earth Sciences

18 Indiana University-Purdue University Indianapolis

19 Indianapolis, IN, 46202, USA

20 Office phone number: 317-274-7764

21 Email: [lxwang@iupui.edu](mailto:lxwang@iupui.edu)

---

This is the author's manuscript of the article published in final edited form as:

Lu, X., Liang, L. L., Wang, L., Jenerette, G. D., McCabe, M. F., & Grantz, D. A. (2017). Partitioning of evapotranspiration using a stable isotope technique in an arid and high temperature agricultural production system. *Agricultural Water Management*, 179, 103–109. <https://doi.org/10.1016/j.agwat.2016.08.012>

## 1 ABSTRACT

2 Agricultural production in the hot and arid low desert systems of southern California  
3 relies heavily on irrigation. A better understanding of how much and to what extent  
4 irrigated water is transpired by crops relative to being lost through evaporation would  
5 improve the management of increasingly limited water resources. In this study, we  
6 examined the partitioning of evapotranspiration (ET) over a field of forage sorghum  
7 (*Sorghum bicolor*), which was under evaluation as a potential biofuel feedstock, based on  
8 isotope measurements of three irrigation cycles at the vegetative stage. This study  
9 employed customized transparent chambers coupled with a laser-based isotope analyzer  
10 to continuously measure near-surface variations in the stable isotopic composition of  
11 evaporation (E,  $\delta_E$ ), transpiration (T,  $\delta_T$ ) and ET ( $\delta_{ET}$ ) to partition the total water flux.  
12 Due to the extreme heat and aridity,  $\delta_E$  and  $\delta_T$  were very similar, which makes this system  
13 highly unusual. Contrary to an expectation that the isotopic signatures of T, E, and ET  
14 would become increasingly enriched as soils became drier, our results showed an  
15 interesting pattern that  $\delta_E$ ,  $\delta_T$ , and  $\delta_{ET}$  increased initially as soil water was depleted  
16 following irrigation, but decreased with further soil drying in mid to late irrigation cycle.  
17 These changes are likely caused by root water transport from deeper to shallower soil  
18 layers. Results indicate that about 46% of the irrigated water delivered to the crop was  
19 used as transpiration, with 54% lost as direct evaporation. This implies that 28 - 39% of  
20 the total source water was used by the crop, considering the typical 60 - 85% efficiency  
21 of flood irrigation. The stable isotope technique provided an effective means of  
22 determining surface partitioning of irrigation water in this unusually harsh production  
23 environment. The results suggest the potential to further minimize unproductive water  
24 losses in these production systems.

- 1 **Keywords:** Biofuel, climate change, drought, ecohydrology, El Centro, Imperial Valley,
- 2 irrigation, water resources, water use efficiency.

# 1 Introduction

2 Agriculture is the largest single user of fresh water globally, accounting for  
3 approximately 70% of the total withdrawn for human consumption (Hoekstra and  
4 Mekonnen, 2012; Wada et al., 2014). In the United States (US), irrigated agriculture is  
5 the second largest primary user of fresh water, accounting for 31% of the developed  
6 water resource (Vörösmarty et al., 2000). The Imperial Valley, in the low elevation desert  
7 of southern California, a region characterized by extreme heat and evaporation, has been  
8 considered a promising area for biofuel feedstock production (Oikawa et al., 2015). This  
9 area produces more than two-thirds of winter vegetables consumed in the US and about  
10 three-quarters of summer hay and other field crops in southern California (Medellín-  
11 Azuara et al., 2012). At present, there is a lack of data addressing the sustainability,  
12 including water use efficiency, of biofuel production in this high temperature agricultural  
13 site.

14 The Colorado River is a key source of water for California's irrigated desert  
15 agriculture, accounting for approximately one-third of annual flow (Cohen et al., 2013).  
16 A growing demand for water, coupled with the limited supplies and impacts of climate  
17 change (Vörösmarty et al., 2000), have placed enormous pressures on California's water  
18 supply. Recent years of drought have exacerbated this water scarcity challenge, especially  
19 in the Imperial Valley.

20 Evapotranspiration (ET) represents one of the largest components of the global water  
21 cycle, with approximately 65% of precipitation returned to the atmosphere via ET at the  
22 global scale (Trenberth et al., 2007). However, ET loss can reach up to 95% in some  
23 dryland systems (Wang et al., 2014; Wilcox and Thurow, 2006). Evapotranspiration

1 consists of two distinct components: evaporation from soil and plant surfaces (E) and  
2 transpiration taken up by roots and lost through stomatal pores (T). These two  
3 components are controlled by different processes and have different water use  
4 implications. Transpiration is controlled by atmospheric evaporative demand and  
5 modified by plant physiological controls on leaf stomata. Because photosynthetic carbon  
6 dioxide fixation is concurrent with water vapor loss, and shares the stomatal diffusion  
7 pathway, irrigated water transpired by crops is productive in that it facilitates  
8 photosynthesis and leads to leaf cooling. Evaporation from soil, in contrast, is not directly  
9 linked to biological processes, but rather results from diffusion of water through the soil  
10 matrix and evaporation at the surface, and is controlled solely by physical factors.  
11 Although it may lead to local evaporative cooling, this water loss is not directly linked to  
12 biological productivity. Because of the different controlling mechanisms, E and T are  
13 likely to have different responses to environmental drivers such as temperature and soil  
14 water content (Kool et al., 2014; Wang et al., 2014). As competition for available  
15 irrigation water increases, a better understanding of how much is transpired relative to  
16 that lost through evaporation, and the factors controlling this partitioning, could  
17 contribute to improved water resource management (Wang and D'Odorico, 2008).

18 Separating E and T has proven to be difficult. Various methods have been proposed,  
19 including empirical measurements and modeling-based approaches. Empirical  
20 measurements can include lysimeters, large tree potometers, whole tree chambers, eddy  
21 covariance measurements of above- and below-canopy fluxes, up-scaling of sap-flow  
22 measurements, and flux-variance similarity partitioning, as well as using stable isotopes  
23 (Kool et al., 2014). Modeling approaches include the FAO-56 dual crop coefficient model

1 (Ding et al., 2013), modeling of canopy and subcanopy fluxes driven by energy balance  
2 measurements (Ershadi et al., 2014; Kalma et al., 2008) or combining process-based  
3 modeling and isotope tracer measurements (Cai et al., 2015; Wang et al., 2015). The  
4 recent development of techniques using stable isotopes of water have provided a useful  
5 tool to separate E and T, that can be applied across broad spatial and temporal scales.  
6 Besides facilitating ET partitioning, the stable isotopic composition of E and T can also  
7 provide insights regarding plant water use dynamics as well as the nature of land-  
8 atmosphere interactions (Parkes et al., 2016).

9 The basis for using the isotopes of H and O in water to partition ET is that  
10 evaporation significantly fractionates the surface soil water, enriching the source with the  
11 heavier isotopes, while transpiration does not lead to fractionation when T is large (Wang  
12 et al., 2012; Wang et al., 2013). Therefore, the isotopic composition of transpiration ( $\delta_T$ )  
13 remains similar to the isotopic composition of the plant source water, while the isotopic  
14 composition of evaporated water differs from that of the source. This results in distinct  
15 isotopic signatures of  $\delta_E$  and  $\delta_T$  (Wang et al., 2013; Zhang et al., 2011).

16 The development of field-deployable laser-based instruments with similar precision  
17 to traditional isotope ratio mass spectrometers (e.g., Wang et al., 2009), has provided a  
18 promising tool to separate T from E in agricultural systems (Wang et al., 2012; Wang et  
19 al., 2013). The application of such methods to direct measurement of the isotopic  
20 composition of E, T and the combination, ET, in a hot, arid agricultural production  
21 system has not previously been attempted.

22 The objectives of the current study are to: (1) use a laser-based isotope analyzer and  
23 customized E and ET chambers to measure the respective isotope signatures,  $\delta_T$ ,  $\delta_E$ , and

1  $\delta_{ET}$ ; (2) combine the estimates of  $\delta_T$ ,  $\delta_E$ ,  $\delta_{ET}$  and total ET to partition the evaporative flux  
2 and to quantify the fraction of irrigation that is partitioned to productive T in this  
3 sorghum production system. These measurements provide important information for  
4 regional water issues, for crop management scenarios, and offer substantial insight into  
5 currently temperate production systems that may become warmer.

## 6 **2 Materials and Methods**

### 7 **2.1 Study site**

8 The study was conducted at the University of California's Desert Research and Extension  
9 Center (DREC) located in the Imperial Valley, southern California (32.867°N  
10 115.448°W) (Fig. 1a). This area is an interior desert valley about 18.3 m below sea level.  
11 The weather represents a desert climate with over 350 days of sunshine. The nearest  
12 automatic weather station (Meloland, 32.806°N 115.446°W) is managed by the  
13 California Management Information System (CIMIS) (<http://www.cimis.water.ca.gov>).  
14 Routine meteorological variables, including solar radiation, wind, humidity, air  
15 temperature, precipitation and soil temperature, as well as reference ET ( $ET_0$ ), have been  
16 recorded hourly since December 1989. The mean annual precipitation from 1990 to 2015  
17 was 80.3 mm year<sup>-1</sup>, while the mean annual  $ET_0$  reaches 1846 mm year<sup>-1</sup> (Fig. 1b). Most  
18 of the rainfall occurs in late summer, with June being the driest month (Fig.1b). The  
19 mean annual temperature is 22.4°C with a monthly mean temperature of 12.6°C in  
20 January and 32.9°C in August (for the period 1990 – 2015) (Fig. 1c). The mean annual  
21 relative humidity of the study area is around 46% (Fig. 1d). The experimental field has  
22 been used for agricultural production since the establishment of DREC in 1912. Irrigation  
23 water is supplied through the All-American Canal, distributed by gravity from the

1 Colorado River. Irrigation is provided by regularly scheduled flooding of furrows. Soils  
2 in the regions are moderately to well-drained deep alluvial soils (42% clay, 41% silt 16%  
3 sand) with sub-surface drainage tile, and pH of 8.3.

4 The *Sorghum bicolor* (cv. Photoperiod LS; Scott Seed Inc.) was planted in February  
5 2012 for biofuel production, and was cut three times each year at the end of the  
6 vegetative stage. Ten extensive field measurements of  $\delta_T$ ,  $\delta_E$  and  $\delta_{ET}$  were conducted on  
7 July 24, 26, 28, 30 and August 4, 6, 7, 13, 18 and 20, 2014. Measurements covered the  
8 three irrigation cycles of one of the three vegetative harvests obtained each year. Plants  
9 were harvested for biomass before substantial flowering had occurred, and thus remained  
10 in the vegetative stage throughout the experiment. The irrigation events occurred on July  
11 22, July 31 and August 9, 2014, each lasting 24 hours. Isotope sampling was conducted  
12 one full day after irrigation to allow for drainage. There were two minor rainfall events  
13 during the measurement period, with a total rainfall of 1.27 mm. The mean monthly air  
14 temperature was 33.5°C and 31.9°C in July and August 2014.

## 15 **2.2 Isotope-based partitioning**

16 The technique developed by Wang et al. (2012; 2013) was modified to fit our  
17 specific needs. The isotopic compositions of the three component vapor fluxes ( $\delta_T$ ,  $\delta_E$  and  
18  $\delta_{ET}$ ) were directly quantified using a field deployable Triple Water Vapor Isotope  
19 Analyzer (T-WVIA, Los Gatos Research, Inc., Mountain View, CA, USA). Samples  
20 were obtained using customized transparent acrylic chambers containing circulation fans  
21 and directly linked as a closed system with the T-WVIA.  $\delta_T$  was measured at 1 Hz with a  
22 customized leaf chamber (2 × 4 × 12 cm) having leaves sealed inside the chamber for 1 to  
23 2 min. The  $\delta_E$  and  $\delta_{ET}$  were measured using a larger customized chamber (50 × 50 × 50



1 cm) placed over bare soil or over areas with both soil and vegetation. Chamber  
 2 measurements were obtained under sunny conditions between 11:00 and 14:00 when  
 3 stomata were as open as soil moisture allowed. This method has been shown to capture  
 4 the short-term variations in  $\delta_T$ ,  $\delta_E$  and  $\delta_{ET}$ , including fast  $\delta_T$  responses to radiation (Wang  
 5 et al., 2012).

6 The fraction of ET partitioned to T is found through measurement of isotopic  
 7 signatures  $\delta_E$ ,  $\delta_T$  and  $\delta_{ET}$ . Assuming a two-component mixing model, the transpired  
 8 fraction of ET is given by:

$$9 \quad \frac{T}{ET} = \frac{\delta_{ET} - \delta_E}{\delta_T - \delta_E}, \quad (1)$$

10 where  $\delta_E$ ,  $\delta_{ET}$ , and  $\delta_T$  are the isotope signatures of E, ET and T, respectively (Wang et  
 11 al., 2010).

12 Keeling plot and mass balance approaches have been used to estimate the isotopic  
 13 composition of vapor fluxes. The Keeling plot approach assumes constant concentration  
 14 and isotopic compositions of the ambient water vapor ( $\delta_A$ ). Source water vapor isotopic  
 15 composition (e.g.,  $\delta_E$ ,  $\delta_T$  or  $\delta_{ET}$ ) was calculated as:

$$16 \quad \delta_M = C_A (\delta_A - \delta_S) \frac{1}{C_M} + \delta_S, \quad (2)$$

17 where  $\delta_M$ ,  $\delta_A$  and  $\delta_S$  are the isotopic compositions of mixed water vapor, ambient water  
 18 vapor and source water vapor in ET, E or T.  $C_M$  is the mixed water vapor concentration  
 19 and  $C_A$  is the ambient water vapor concentration at the measurement location (Wang et  
 20 al., 2010).

21 The calculation of source water vapor isotopic composition using a mass balance  
 22 approach was given as:

$$s = \frac{C_{M1} C_{A1}}{C_M C_{A2}}, \quad (3)$$

3 Under our measurement conditions, the maximum concentration of water vapor  
4 before condensation occurred in August was 49,100 ppm. Measurements were terminated  
5 when water concentration approached 45,000 ppm in order to prevent condensation. The  
6  $\delta_E$ ,  $\delta_T$  and  $\delta_{ET}$  were measured at random locations with four repeated measurements from  
7 each sampling time. Data were excluded due to instrumental malfunction and obvious  
8 data errors (e.g., the fraction of ET is greater than 1 or less than 0). ET partitioning was  
9 not possible for August 13, August 18, and August 20, as chamber-based  $\delta_{ET}$  were not  
10 available. Both  $\delta^{18}O$  and  $\delta D$  data were used to demonstrate the temporal changes in  
11  $\delta_E$ ,  $\delta_T$  or  $\delta_{ET}$ , while only  $\delta D$  data were used for ET partitioning.

### 12 **2.3 Total ET measurements**

13 Total ET was monitored at 10 Hz using the eddy-covariance technique via an open-  
14 path infrared gas analyzer (IRGA) (Li7500, LI-COR, Lincoln, NE, USA) and a 3-D sonic  
15 anemometer (CSAT3, CSI, Logan, Utah, USA) (Oikawa et al., 2015). The instrument  
16 was mounted on a tower located within 10 m of the chamber measurements, at a height of  
17 2.5 meters above the canopy. Data processing was conducted in EddyPro 5.2 (LI-COR,  
18 Lincoln, NE, USA) and followed standard flux calculations over 30 min intervals. The  
19 footprint of the tower was determined using an approximate analytical model (Hsieh et  
20 al., 2000). Evapotranspiration fluxes with 70% of the footprint exceeding the edge of the  
21 field were removed. The ET data were gap-filled following Reichstein et al. (2005).

## 22 **3 Results**

1 This study was conducted under extremely hot and arid conditions (Fig. 1). Fig. 2 shows  
2 the hydrogen and oxygen isotopes in the evaporation and transpiration waters. The  $\delta^{18}\text{O}$   
3 of transpiration water ( $\delta_{\text{T}}$ ) ranged from -6.07 to 6.99‰, with a mean value of 0.04‰ and  
4 standard deviation of 3.60‰, while  $\delta\text{D}$  of  $\delta_{\text{T}}$  ranged from -89.75 to -70.44‰, with a  
5 mean value of -83.27‰ and standard deviation of 7.28‰ (Fig. 2). The least squares  
6 fitting between  $\delta\text{D}$  and  $\delta^{18}\text{O}$  in transpiration was:  $\delta\text{D} = 1.4 \times \delta^{18}\text{O} - 83.3$  ( $R^2 = 0.47$ ,  $p <$   
7  $0.05$ ). The  $\delta^{18}\text{O}$  of evaporation water ( $\delta_{\text{E}}$ ) ranged from -4.99 to 5.10‰, with a mean value  
8 of -1.35‰ and standard deviation of 3.52‰, while  $\delta\text{D}$  of  $\delta_{\text{E}}$  ranged from -97.33 to -  
9 71.07‰, with a mean value of -83.48‰ and standard deviation of 8.39‰ (Fig. 2). The  
10 least squares fitting between  $\delta\text{D}$  and  $\delta^{18}\text{O}$  in evaporation was:  $\delta\text{D} = 1.5 \times \delta^{18}\text{O} - 82.0$  ( $R^2$   
11  $= 0.38$ ,  $p < 0.05$ ). The local meteoric water line (LMWL) determined via least squares  
12 fitting of the irrigation water isotopic values was:  $\delta\text{D} = 7.3 \times \delta^{18}\text{O} + 3.6$ .

13 All  $\delta_{\text{E}}$  values fell to the right side of the irrigation water line, revealing a strong  
14 evaporation effect on  $\delta_{\text{E}}$  (Fig. 2). The  $\delta\text{D}$ - $\delta^{18}\text{O}$  regression lines for both  $\delta_{\text{T}}$  and  $\delta_{\text{E}}$  deviated  
15 substantially from the LMWL, producing very negative values of deuterium excess (d-  
16 excess: defined as  $\text{d-excess} = \delta\text{D} - 8.0 \times \delta^{18}\text{O}$ ) of  $\delta_{\text{T}} = -83.3$  and  $\delta_{\text{E}} = -82.0$ ‰. Although  
17 such negative d-excess values are not commonly seen, the values are comparable to those  
18 obtained in a recent study in one of the driest regions in China. In that study, a negative  
19 d-excess value of -85.6‰ in leaf water was reported (Zhao et al., 2014). In the present  
20 study, the slopes of the  $\delta\text{D}$ - $\delta^{18}\text{O}$  regression lines for  $\delta_{\text{T}}$  and  $\delta_{\text{E}}$  were much lower than 8.0,  
21 suggesting substantial water loss through direct evaporation and transpiration drawn from  
22 isotopically enriched soil water. Moreover, the intersections of  $\delta\text{D}$ - $\delta^{18}\text{O}$  regression lines

1 for  $\delta_T$  and  $\delta_E$  and irrigation water line fell within the range of the isotopic compositions of  
2 irrigation waters, supporting an E and T origin from this source (Fig. 2).

3 In contrast to an expectation that the isotopic signatures of T, E, and ET would  
4 become increasingly enriched as soils became drier, our results present a more complex  
5 pattern. Here, the isotopic signatures of E, T and ET increased (less negative) initially as  
6 water was depleted, but then decreased at the end of each irrigation cycle (Fig. 3a and b).  
7 Both  $\delta D$  and  $\delta^{18}O$  followed similar patterns and it was replicated in all three irrigation  
8 cycles (Fig. 3a and b).

9 ET partitioning was calculated using a simple 2-source model, as defined in Equation  
10 1. It was estimated that about  $46\% \pm 5.6\%$  of the irrigated water was used as transpiration  
11 by crops after runoff as tailwater and drainage, while 54% was lost as direct evaporation  
12 from the soil (Table 1). Transpiration between May and October 2014 ranged from 0.59  
13 to 6.08 mm/day, with a mean value of 3.04 mm/day (Fig. 4). Both T/ET and LAI  
14 increased as the crop developed (Fig. 5a) during the vegetation stage and the relationship  
15 between T/ET and LAI was  $T/ET=0.45 \times LAI^{0.19}$  (Fig. 5b).

## 16 **4 Discussion**

17 An increasing number of studies have used the stable isotope technique to separate ET  
18 components, and predict ET partitioning changes under both agricultural and natural  
19 settings. Here we present one of the first studies testing the field application of a chamber  
20 method to directly measure isotopic composition of all three components (E, T and ET),  
21 in an extreme agricultural production environment. By using this approach, we could also  
22 predict the patterns of plant water use based on the changes of transpiration isotopic  
23 composition. Particularly we monitored the plant water use pattern at the vegetative

1 stage. Water loss by evaporation can be much higher at the vegetative stage than the later  
2 growing stages (Wang et al., 2014), so any improvement of water management is critical  
3 at this stage.

4 Of particular interest was the examination of these evaporative processes under  
5 extremely hot and arid condition, with local conditions having a mean  $ET_o$  more than 20  
6 times the mean annual precipitation. Due to the extreme heat and aridity,  $\delta_E$  and  $\delta_T$  were  
7 very similar, which is rarely seen in the literature and mark this system as quite unique  
8 (see Fig. 6). The small difference between  $\delta_T$  and  $\delta_E$  makes it challenging to accurately  
9 discriminate the isotopic compositions of these two fluxes, and ultimately to partition  
10 total ET into relative rates of E and T. Despite this complexity, our chamber method  
11 generally worked well for  $\delta_T$ ,  $\delta_E$ , and  $\delta_{ET}$  estimates, based on agreement between the  
12 Keeling plot and mass balance approaches (Appendix Fig. S1).

13 Our results yield interesting insights into how isotopic signatures of T, E and ET can  
14 change with depletion of water within the irrigation cycles. Contrary to an expectation  
15 that the isotopic signatures of T, E, and ET would continuously become enriched as soils  
16 became drier, we have observed that the isotopic signatures of E, T and ET increased as  
17 water was depleted, but decreased at the end of each irrigation cycle. The observed  
18 pattern of depleted isotopic signatures of T, E, and ET in mid to late irrigation cycles  
19 might be caused by lateral roots accessing water from deeper soil depths when shallow  
20 water is reduced, redistributing the deeper water to shallower layers (Ahmed et al., 2016;  
21 Stone et al., 2001). The root system of maize, a related  $C_4$  grass, consists of pre-  
22 embryonic primary and seminal roots formed during embryogenesis and lateral roots  
23 formed during post-embryonic development (Ahmed et al., 2016). A recent study using

1 neutron radiography to examine the mechanism of maize root water uptake has found that  
2 the function of lateral roots is to uptake water from the soil while the function of primary  
3 and seminal roots is to axially transport water to the shoot (Ahmed et al., 2016). As  
4 sorghum has similar root water uptake dynamics to corn (Srayeddin and Doussan, 2009),  
5 this rooting mechanism might explain why the isotopic signatures of E, T, and ET  
6 increase but then decrease within the irrigation cycles. As sorghum roots grow steadily  
7 throughout the season, when the shallow water is depleted and soil dries, the lateral roots  
8 could extract water from the subsoil and redistribute to the surface layer for transpiration  
9 and evaporation, leading to isotopic depletion of E, T and ET.

10 Other factors such as soil properties and precipitation could also influence the  
11 isotopic compositions of different components and ET amount. The small precipitation  
12 events occurring on August 2 and August 3, 2014 likely caused a higher value of  $\delta_E$  on  
13 Aug 4 and 6 (Fig. 5) due to a strong evaporation of the rainfall on surface soil. The  $\delta_T$  is  
14 lower than  $\delta_E$  for these two cases because transpiration response is likely damped due to  
15 the crop water use from deeper soil layers, in addition to the use of limited surface  
16 rainfall water. The daily average soil moisture varies between 0.17 and 0.42  $\text{cm}^3 \text{cm}^{-3}$   
17 (Oikawa et al., 2014), and all samplings were conducted after irrigation when the field is  
18 still at field capacity.

19 Transpiration values measured at our site were comparable to those measured in  
20 other dryland agriculture sites. However, the ratio of transpiration to evapotranspiration  
21 (T/ET) was considerably lower. For example, a study in China found that the measured T  
22 ranged from 1.02 to 4.91 mm/day, accounting for 60% to 83% of the total ET (Zhang et  
23 al., 2011). Based on this study, the ratio of transpiration to evapotranspiration (T/ET)

1 slightly increased with the increasing trend of leaf area index (LAI) as crops develop  
2 (Fig. 5), and the relationship between T/ET and LAI from our study is in-between those  
3 reported in previous study for early season and peak LAI stage (Wang et al., 2014). We  
4 have estimated that the rate of evaporation could be as high as 54% at the vegetative  
5 stage, thus it may be possible to improve water use efficiency of sorghum at the early  
6 growing stage in such systems with extremely limited water resources. The vegetative  
7 stage may play a dominant role in seasonal T/ET (Kang et al., 2003; Wang et al., 2014),  
8 particularly in forage and lignocellulosic biofuel systems which remain in the vegetative  
9 stage. Our measurements from one vegetative harvest cycle may be representative of the  
10 water use dynamics of the entire growing season.

11 Like many crops in the Imperial Valley, the forage sorghum evaluated here was  
12 irrigated through flooding of furrows. Compared to the other irrigation systems such as  
13 drip and spray irrigation, flood irrigation exhibits some inefficiencies due to surface  
14 runoff, deep percolation and unproductive evaporative losses (Cooley et al., 2009).  
15 However, flood systems have advantages such as simplicity of design, low capital  
16 investment, and low energy requirement. Deep drainage to the tile system is critical in  
17 this environment to leach salts that are accumulated from the irrigation water (Oikawa et  
18 al., 2015). The Colorado River, at the point of interception of the All American Canal,  
19 has a salinity of 879 mg L<sup>-1</sup> TDS (Forum, 2011).

20 It has been estimated that the potential irrigation efficiency (defined as the volume of  
21 water used by the plant divided by the volume of irrigation water applied to the field  
22 minus changes in surface and soil storage) for flood irrigation systems ranges from 60 –  
23 85% (Cooley et al., 2009). Combining the current analysis and the typical efficiency of

1 flood irrigation system, the amount of water used by the plant via transpiration relative to  
2 the amount of water delivered to the field in this case ranged from 28 - 39%. This  
3 indicates that although the production of biofuel feedstock is extremely high under the  
4 climate and soil conditions of this region (Oikawa et al., 2015), the water use and water  
5 use efficiency may need to be taken into consideration for the sake of sustainability.

## 6 **5 Conclusions**

7 This study presents a novel application of the combined use of customized chambers  
8 and a laser-based isotope analyzer to directly quantify isotopic signatures of T, E and ET  
9 *in situ* and examine ET partitioning over a field of forage sorghum in an extreme field  
10 condition. As a consequence of strong evaporation under extreme heat and arid  
11 conditions, the studied system showed similar  $\delta_T$  and  $\delta_E$  values, which is rarely seen in  
12 the literature and increases the difficulty in discriminating isotopic signatures and to  
13 partition ET. The strong evaporative gradient in this ecosystem was supported by the fact  
14 of very low slopes of  $\delta D$  and  $\delta^{18}O$  relationship for both  $\delta_T$  and  $\delta_E$ .

15 The results revealed an interesting pattern of the isotopic signatures of E, T, and ET.  
16 All components increased as the soil dried, but decreased at the mid to end of each  
17 irrigation cycle. These changes were likely a result of the lateral roots extracting water  
18 from the subsoil and redistribution to the surface layer, so both crop and surface soil  
19 evaporation would access water from deeper layers when the shallow water is depleted.

20 For the studied ecosystem, approximately 46% of the irrigated water delivered to the  
21 crops was transpired, with 54% was lost via direct evaporation from the soil during the  
22 vegetative stage. Considering inherent irrigation inefficiencies, approximately 28 - 39%



1 of the total source water was used by crops, suggesting potential for improved water use  
2 efficiency.

### 3 **Acknowledgements**

4 We acknowledge the support by USDA-NIFA Award No. 2011-67009-30045 and  
5 partial support from the U.S. National Science Foundation (IIA-1427642 and EAR-  
6 155489). Matthew McCabe was supported by funding from the King Abdullah University  
7 of Science and Technology. We thank Dr. Yucui Zhang and one anonymous reviewer for  
8 their valuable comments, which greatly improved the quality of the manuscript.

### 9 **References**

- 10 Ahmed, M.A., Zarebanadkouki, M., Kroener, E., Kaestner, A., Carminati, A., 2016.  
11 Measurements of water uptake of maize roots: the key function of lateral roots. *Plant Soil*  
12 398, 59-77.  
13  
14 Cai, M.Y., Wang, L., Parkes, S.D., Strauss, J., McCabe, M.F., Evans, J.P., Griffiths,  
15 A.D., 2015. Stable water isotope and surface heat flux simulation using ISOLSM:  
16 evaluation against in-situ measurements. *Journal of Hydrology* 523, 67-78.  
17  
18 Cohen, M., Christian-Smith, J., Berggren, J., 2013. *Water to Supply the Land*.  
19  
20 Cooley, H., Christian-Smith, J., Gleick, P.H., 2009. *Sustaining California agriculture in*  
21 *an uncertain future*.  
22  
23 Ding, R., Kang, S., Zhang, Y., Hao, X., Tong, L., Du, T., 2013. Partitioning  
24 evapotranspiration into soil evaporation and transpiration using a modified dual crop  
25 coefficient model in irrigated maize field with ground-mulching. *Agricultural water*  
26 *management* 127, 85-96.  
27  
28 Ershadi, A., McCabe, M.F., Evans, J.P., Chaney, N.W., Wood, E.F., 2014. Multi-site  
29 evaluation of terrestrial evaporation models using FLUXNET data. *Agric. For. Meteorol.*  
30 187, 46-61.  
31  
32 Forum, C.R.B.S.C., 2011. *Water Quality Standards for Salinity Colorado River System*  
33 Hoekstra, A.Y., Mekonnen, M.M., 2012. The water footprint of humanity. *Proceedings of*  
34 *the national academy of sciences* 109, 3232-3237.

1 Hsieh, C.I., Katul, G., Chi, T.W., 2000. An approximate analytical model for footprint  
2 estimation of scalar fluxes in thermally stratified atmospheric flows. *Advances in Water*  
3 *Resources* 23, 765-772.  
4  
5 Kalma, J., McVicar, T., McCabe, M., 2008. Estimating land surface evaporation: A  
6 review of methods using remotely sensed surface temperature data. *Surveys in*  
7 *Geophysics* 29, 421-469.  
8  
9 Kang, S., Gu, B., Du, T., Zhang, J., 2003. Crop coefficient and ratio of transpiration to  
10 evapotranspiration of winter wheat and maize in a semi-humid region. *Agricultural water*  
11 *management* 59, 239-254.  
12  
13 Kool, D., Agam, N., Lazarovitch, N., Heitman, J.L., Sauer, T.J., Ben-Gal, A., 2014. A  
14 review of approaches for evapotranspiration partitioning. *Agric. For. Meteorol.* 184, 56-  
15 70.  
16  
17 Medellín-Azuara, J., Vergati, J.A., Sumner, D.A., Howitt, R.E., Lund, J.R., 2012.  
18 Analysis of effects of reduced supply of water on agricultural production and irrigation  
19 water use in Southern California.  
20  
21 Oikawa, P.Y., Gratz, D.A., Chatterjee, A., Eberwein, J.E., Allsman, L.A., Jenerette, G.D.,  
22 2014. Unifying soil respiration pulses, inhibition, and temperature hysteresis through  
23 dynamics of labile carbon and soil O<sub>2</sub>. *J. Geophys. Res.-Biogeo* 115, 521-536.  
24  
25 Oikawa, P.Y., Jenerette, G.D., Grantz, D.A., 2015. Offsetting high water demands with  
26 high productivity: Sorghum as a biofuel crop in a high irradiance arid ecosystem. *GCB*  
27 *Bioenergy* 7, 974-983.  
28  
29 Parkes, S.D., McCabe, M.F., Griffiths, A.D., Wang, L., Chambers, S., Ershadi, A.,  
30 Williams, A.G., Strauss, J., Element, A., 2016. Response of water vapour D-excess to  
31 land-atmosphere interactions in a semi-arid environment. *Hydrol. Earth Syst. Sci.*  
32 *Discuss.*  
33  
34 Reichstein, M., Falge, E., Baldocchi, D., Papale, D., Aubinet, M., Berbigier, P.,  
35 Grünwald, T., 2005. On the separation of net ecosystem exchange into assimilation and  
36 ecosystem respiration: review and improved algorithm. *Glob. Change Biol.* 11, 1424-  
37 1439.  
38  
39 Srayeddin, I., Doussan, C., 2009. Estimation of the spatial variability of root water uptake  
40 of maize and sorghum at the field scale by electrical resistivity tomography. *Plant Soil*  
41 319, 185-207.  
42  
43 Stone, L.R., Goodrum, D.E., Jaafar, M.N., Khan, A.H., 2001. Rooting front and water  
44 depletion depths in grain sorghum and sunflower. *Agronomy Journal* 93, 1105-1110.

1 Trenberth, K.E., Smith, L., Qian, T., Dai, A., Fasullo, J., 2007. Estimates of the global  
2 water budget and its annual cycle using observational and model data. *Journal of*  
3 *Hydrometeorology* 8, 758–769.  
4  
5 Vörösmarty, C.J., Green, P., Salisbury, J., Lammers, R.B., 2000. Global water resources:  
6 vulnerability from climate change and population growth. *Science* 289, 284-288.  
7  
8 Wada, Y., Wisser, D., Bierkens, M.F.P., 2014. Global modeling of withdrawal, allocation  
9 and consumptive use of surface water and groundwater resources. *Earth System*  
10 *Dynamics* 5, 15-40.  
11  
12 Wang, L., Caylor, K., Dragoni, D., 2009. On the calibration of continuous, high-precision  
13  $\delta^{18}\text{O}$  and  $\delta^2\text{H}$  measurements using an off-axis integrated cavity output spectrometer  
14 *Rapid Communications in Mass Spectrometry* 23, 530-536.  
15  
16 Wang, L., Caylor, K.K., Villegas, J.C., Barron-Gafford, G.A., Breshears, D.D., Huxman,  
17 T.E., 2010. Evapotranspiration partitioning with woody plant cover: assessment of a  
18 stable isotope technique. *Geophysical Research Letters* 37, L09401.  
19  
20 Wang, L., D'Odorico, P., 2008. The limits of water pumps. *Science* 321, 36-37.  
21  
22 Wang, L., Good, S.P., Caylor, K.K., 2014. Global synthesis of vegetation control on  
23 evapotranspiration partitioning. *Geophysical Research Letters* 41, 6753–6757.  
24  
25 Wang, L., Good, S.P., Caylor, K.K., Cernusak, L.A., 2012. Direct quantification of leaf  
26 transpiration isotopic composition. *Agric. For. Meteorol.* 154-155, 127-135.  
27  
28 Wang, L., Niu, S., Good, S., Soderberg, K., Zhou, X., Xia, J., Sherry, R., Luo, Y., Caylor,  
29 K., McCabe, M., 2013. The effect of warming on grassland evapotranspiration  
30 partitioning using laser-based isotope monitoring techniques. *Geochimica et*  
31 *Cosmochimica Acta* 111, 28-38.  
32  
33 Wang, P., Yamanaka, T., Li, X.Y., Wei, Z., 2015. Partitioning evapotranspiration in a  
34 temperate grassland ecosystem: Numerical modeling with isotopic tracers. *Agric. For.*  
35 *Meteorol.* 208, 16-31.  
36  
37 Wilcox, B.P., Thurow, T.L., 2006. Emerging issues in rangeland ecohydrology:  
38 vegetation change and the water cycle. *Rangeland Ecology & Management* 59, 220–224.  
39  
40 Zhang, Y., Shen, Y., Sun, H., Gates, J.B., 2011. Evapotranspiration and its partitioning in  
41 an irrigated winter wheat field: A combined isotopic and micrometeorologic approach.  
42 *Journal of Hydrology* 408, 203-211.  
43  
44 Zhao, L., Wang, L., Liu, X., Xiao, H., Ruan, Y., Zhou, M., 2014. The patterns and  
45 implications of diurnal variations in the d-excess of plant water, shallow soil water and  
46 air moisture. *Hydrology and Earth System Sciences* 18, 4129-4151.

1 Table 1. Evapotranspiration partitioning calculations at representative sampling dates.  
2

<b>Date</b>	<b>%T</b>	<b>%E</b>
<b>7/24/2014</b>	40.2	59.8
<b>7/28/2014</b>	39.3	60.7
<b>7/30/2014</b>	51.8	48.2
<b>8/4/2014</b>	47.3	52.7
<b>8/6/2014</b>	52.3	47.7
<b>8/7/2014</b>	45.0	55.0
<b>Mean</b>	<b>46.0</b>	<b>54.0</b>
<b>SD</b>	<b>5.6</b>	<b>5.6</b>

3

4 Note: SD refers to standard deviation.

5

6

7

## 1 **Figure Legends**

2 **Figure 1.** Location of the University of California Desert Research and Extension Center  
3 (DREC). Monthly mean precipitation (mm), reference evapotranspiration ( $ET_o$ ) (mm),  
4 temperature and relative humidity over 1990 – 2015 for the Meloland station of the  
5 California Irrigation Management Information System (CIMIS), located within a few  
6 hundred meters of the experimental field.

7

8 **Figure 2.** The  $\delta D$ - $\delta^{18}O$  relationships of leaf transpiration ( $\delta_T$ , blue circles) and soil  
9 evaporation ( $\delta_E$ , red circles). Black circles depict the measured isotopic composition of  
10 the irrigation water. The dashed black line is the Local Meteoric Water Line, determined  
11 via least-squares fitting of the irrigated water isotope values. The solid gray line is the  
12 Global Meteoric Water Line (GMWL). VSMOW is Vienna Standard Mean Ocean Water.

13

14 **Figure 3.** Patterns of deuterium and oxygen isotope signatures for transpiration (T),  
15 evaporation (E) and evapotranspiration (ET) over the three irrigation cycles. (a) observed  
16 pattern for deuterium ( $\delta D$ ), (b) observed pattern for oxygen ( $\delta^{18}O$ ). VSMOW stands for  
17 Vienna Standard Mean Ocean Water.

18

19 **Figure 4.** Daily variation of transpiration (T) and evapotranspiration (ET) during the  
20 vegetative stage, calculated by combing isotope partitioning and total ET results obtained  
21 from concurrent eddy covariance measurements.

1 **Figure 5.** Variations of leaf area index (LAI) during crop development (a) and the  
2 relationship between T/ET and LAI (b).

3

4 **Figure 6.** Comparison of deuterium isotope signature of leaf transpiration ( $\delta_T$ ) and soil  
5 evaporation ( $\delta_E$ ) over the measurement period. VSMOW stands for Vienna Standard  
6 Mean Ocean Water.

7

8

9

10

11

12

13

14

15

16

17

18

19

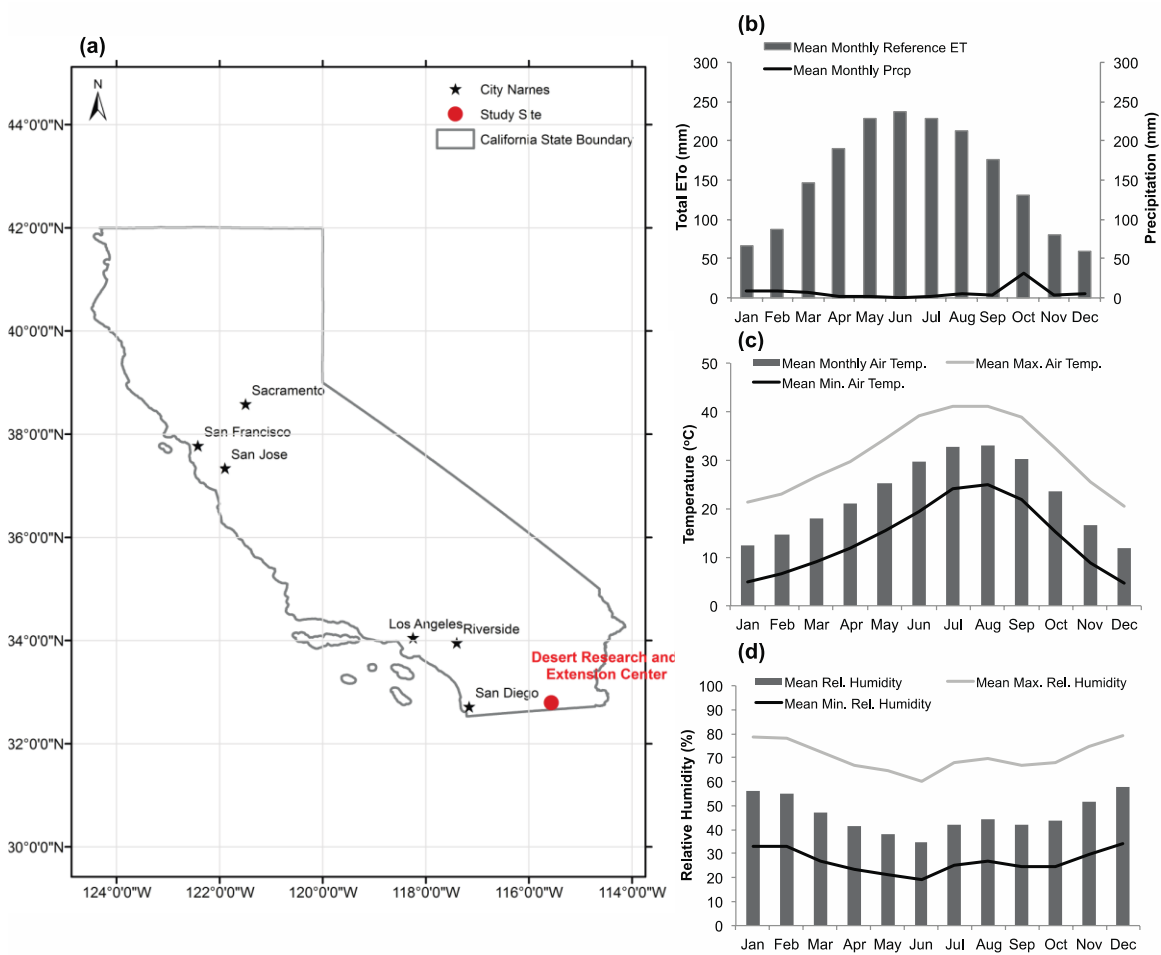
20

21

22

23

# 1 Figures



2

3 **Figure 1**

4

5

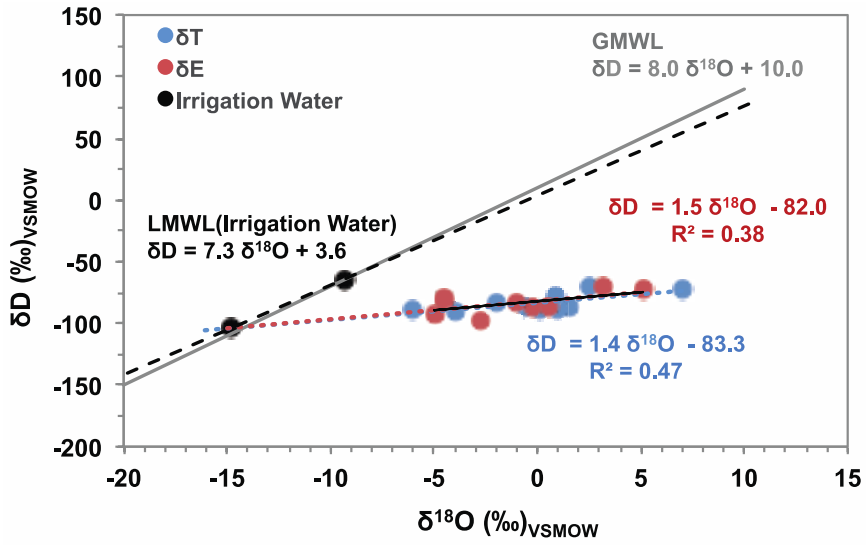
6

7

8

9

10



1

2 **Figure 2**

3

4



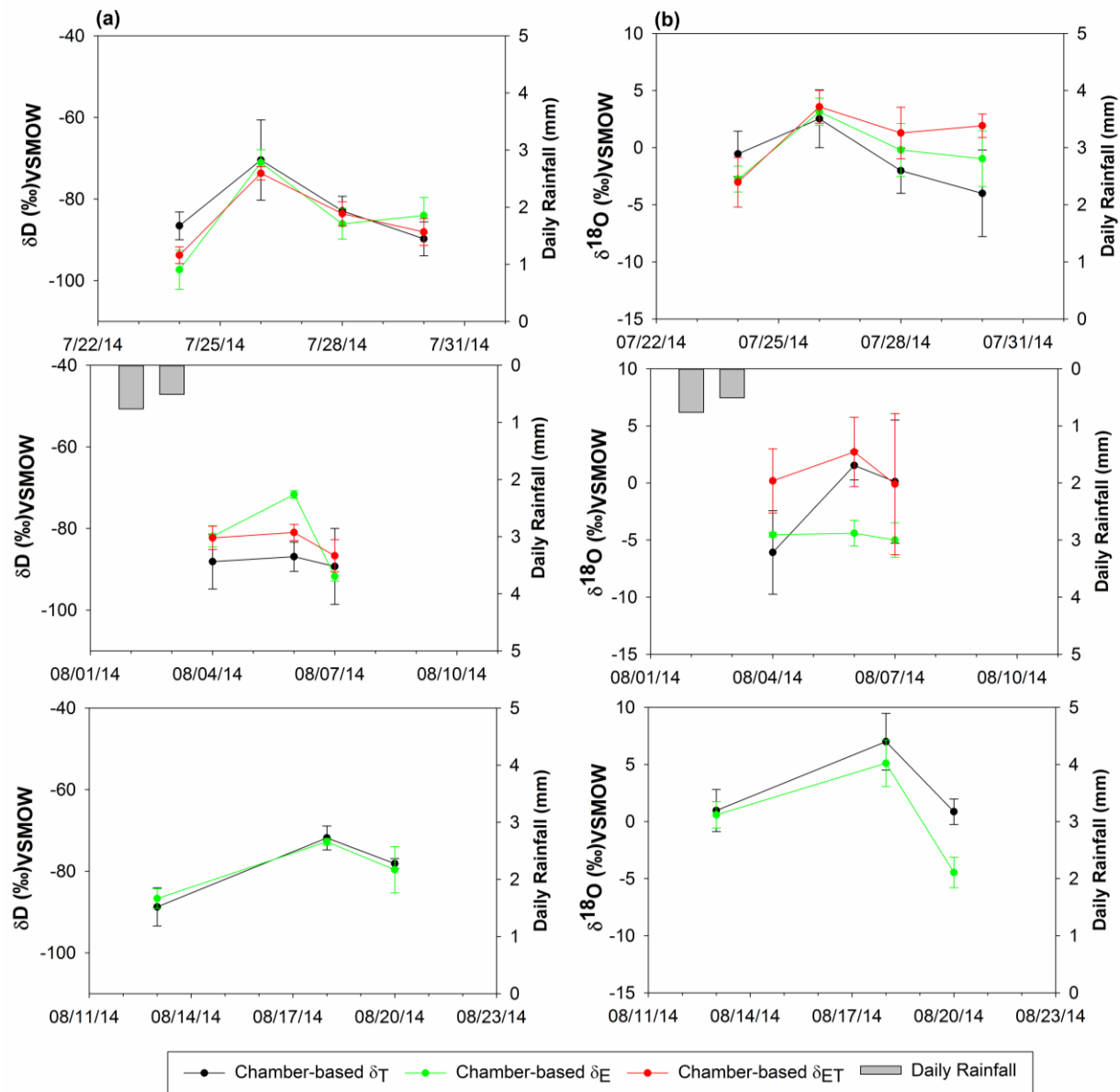
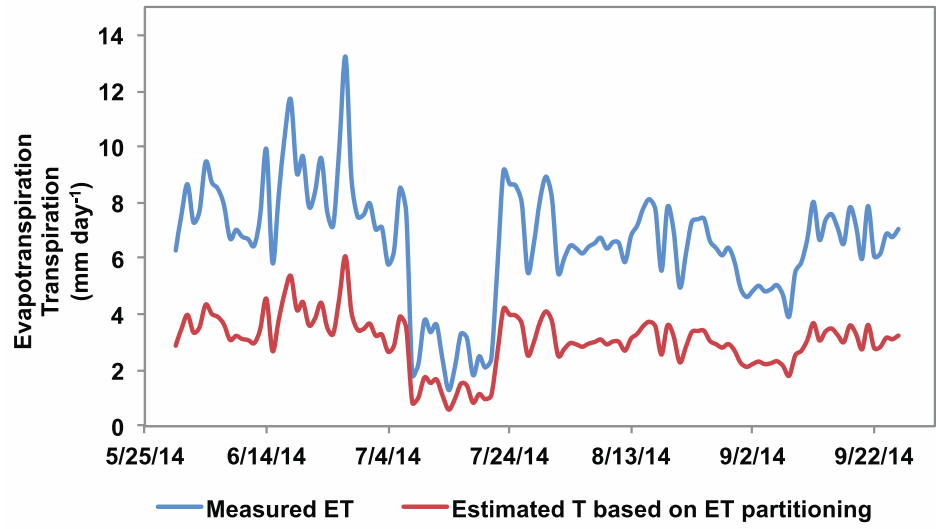


Figure 3



**Figure 4**

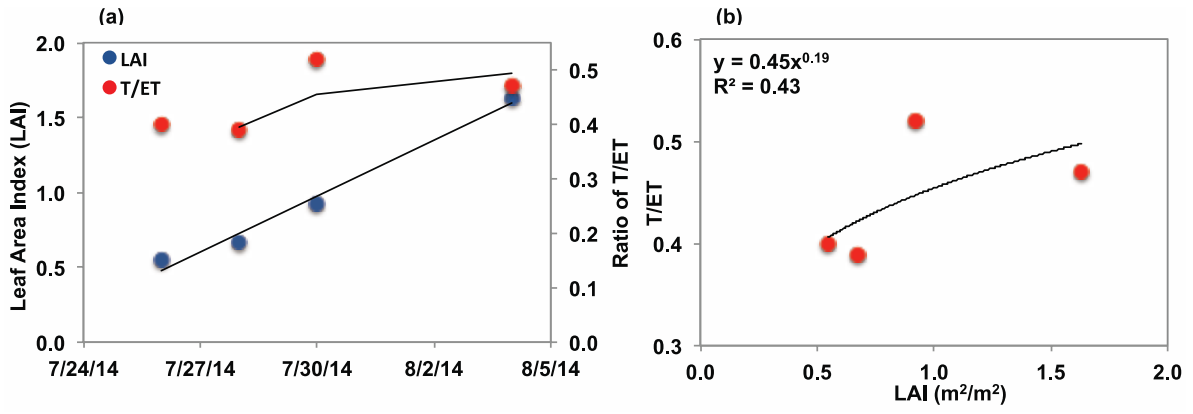
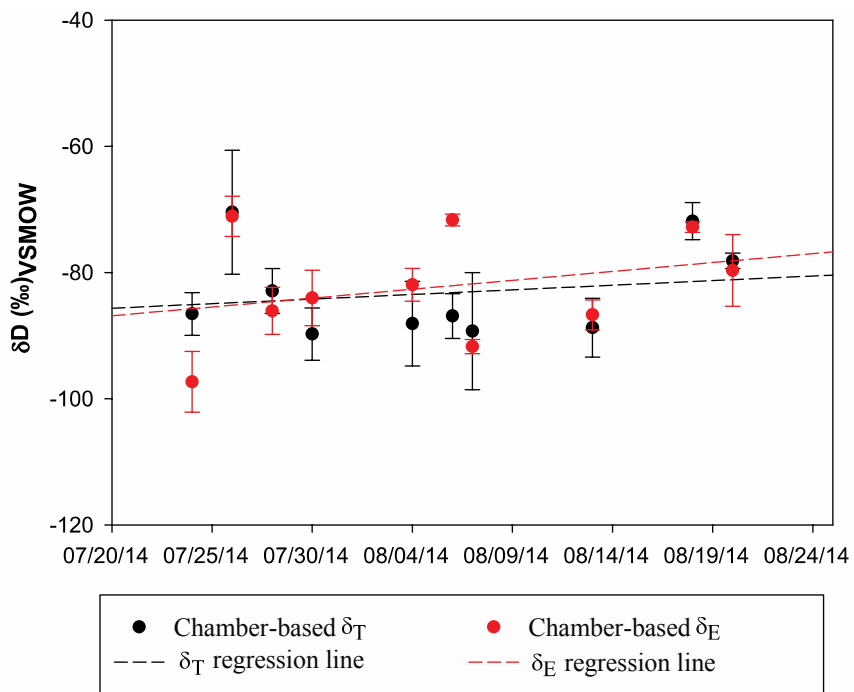


Figure 5



**Figure 6**